Assignment 1

BEM Wind Turbine

Carlos Espinós Garcia
Niklas Perujo
Bernat Serra Zueras

Rotor and Wake Aerodynamics

TU Delft

Contents

1

Introduction

1.1. Assignment BEM BERNAT

Blabla

1.2. Single polar innacuraciesBERNAT

Chowchow

2

Blade Element Momentum theory

2.1. Main assumptions of the BEM theory NIKLAS

Perujo

2.2. Code flow chart CARLOS

The code structure for solving the BEM equations in one cell at a given azimuth and radius is explained below.

1. First guess for the flow induction factors: $a_0 = 1/3$ and $a'_0 = 0$.
2. Forces estimation.
   (a) The local velocities to the given azimuth and radius are calculated.
      i. The yaw flow correction constant is estimated: $\chi = (0.6a + 1)\gamma$ and $K = 2\tan 1/2\chi$.
      ii. Axial velocity: $u_a = \cos\gamma - a(1 + K\mu\sin\psi)$.
      iii. Tangential velocity: $u_t = \lambda\mu(1 + a') - \sin\gamma\cos\psi$.
   (b) Flow angle determination from the local velocities: $\tan\phi = u_a/u_t$.
   (c) Angle of attack is determined from the flow angle ϕ and blade geometry: $\alpha = \phi - \beta$.
   (d) Aerodynamic coefficients c_l and c_d are obtained from airfoil polar curve.
   (e) The forces are estimated using the Blade Element Theory.
      i. Axial force: $F_x = 1/2(u_a^2 + u_t^2)(c_l\cos\phi + c_d\sin\phi)cB\Delta\phi/2\pi$.
      ii. Tangential force: $F_t = 1/2(u_a^2 + u_t^2)(c_l\sin\phi - c_d\cos\phi)cB\Delta\psi/2\pi$.
3. Induction factors estimation.
   (a) Cell surface: $dS = r\Delta r\Delta\psi$.
   (b) Prandtl's loss factor: $f(\mu) = 2/\pi\arccos\left[\exp\left(-B/2\left((1-\mu)/\mu\right)\sqrt{1 + (\lambda^2\mu^2)/((1-a)^2)}\right)\right]$.
   (c) Axial induction factor.
      i. Thrust coefficient: $C_T = F_x/(1/2u_\infty^2\Delta S)$.
      ii. Thrust coefficient limit for applying Glauert correction for heavily loaded rotors: $C_{T_2} = 2\sqrt{C_{T_1}} - C_{T_1}$, where $C_{T_1} = 1.816$.
      iii. If $C_T < C_{T_2}$, $a = 1/2 - 1/2\sqrt{1 - C_T}$.
      iv. If $C_T \geq C_{T_2}$, $a = 1 + (C_T - C_{T_1})/(4\sqrt{C_{T_1} - 4})$.
   (d) Tangential induction factor.
      i. Tangential force coefficient: $C_{F_t} = F_t/(1/2u_\infty^2\Delta S)$.

ii. Tangential induction factor: $a' = C_{F_t}/(4a(1-a)\lambda\mu)$.

(e) Correct the flow induction factors with Prandtl's loss factor: $a = a/f$ and $a' = a'/f$.

4. Convergence check.

(a) Esimtate the error: $e = max(|a - a_0|, |a' - a'_0|)$.

(b) If the error is larger than the tolerance, the process is repeated from step 2 with $a_0 = 0.75a_0 + 0.25a$ and $a'_0 = 0.75a'_0 + 0.25a'$.

(c) If the error is smaller than the tolerance, the calculation has converged.

3

Results

Describe the initial conditions, table, cool

3.1. BEM alligned rotor BERNAT

3.1.1. Main outputs BERNAT

Angle of attack and inflow angle BERNAT
Axial and azimuthal inductions BERNAT
Thrust and azimuthal loading BERNAT
Total thrust and torque BERNAT

3.2. BEM yawed rotor NIKLAS

3.2.1. Main outputs NIKLAS

Angle of attack and inflow angle NIKLAS
Axial and azimuthal inductions NIKLAS
Thrust and azimuthal loading NIKLAS
Total thrust and torque NIKLAS

3.3. Influence of the tip correction CARLOS

The results shown in this section were obtained for the rotor described in the assignment instructions, operating with a tip speed ratio $\lambda = 8$ and no yaw. It can be seen that the tip correction reduces the power and thrust, resulting in a worse performance. Indeed, the rotor without the tip correction has a higher C_P/C_T ratio.

Near the blade tip, the flow angle ϕ is reduced due to the tip vortex (Figure 3.1), because it induces a larger axial velocity (Figure 3.3). Having a lower flow angle ϕ results in a reduced power extraction, which is proportional to $c_l \sin\phi - c_d \cos\phi$ (Figure 3.4) [1]. However, reducing the flow angle ϕ contributes to an increase of the thrust, since it is proportional to $c_l \cos\phi + c_d \sin\phi$.

Note that c_l also decreases due to the reduction of ϕ, because it implies a decrease of the angle of attack α (Figure 3.2). Moreover, the relative velocity, which also affects the loads, will also be larger for the case without tip correction.

The tip correction tries to account for this effect. The expression Prandtl derived for that factor is shown in equation 3.1. Its value over the blade is plotted in Figure 3.5. It relates the induction factor near the blade a_b with the azimuth average a: $a_b = a/f$ [1].

$$f(\mu) = \frac{2}{\pi}\arccos\left[\exp\left(-\frac{B}{2}\left(\frac{1-\mu}{\mu}\right)\sqrt{1+\frac{\lambda^2\mu^2}{(1-a)^2}}\right)\right] \tag{3.1}$$

- Power coefficient C_P
  - Tip correction: 0.4528
  - No tip correction: 0.4757

  - Increase: 5.05 %

- Thrust coefficient C_T
  - Tip correction: 0.6581
  - No tip correction: 0.6691
  - Increase: 1.67 %

- Power to thrust ratio C_P/C_T
  - Tip correction: 0.6880
  - No tip correction: 0.7109
  - Increase: 3.32 %

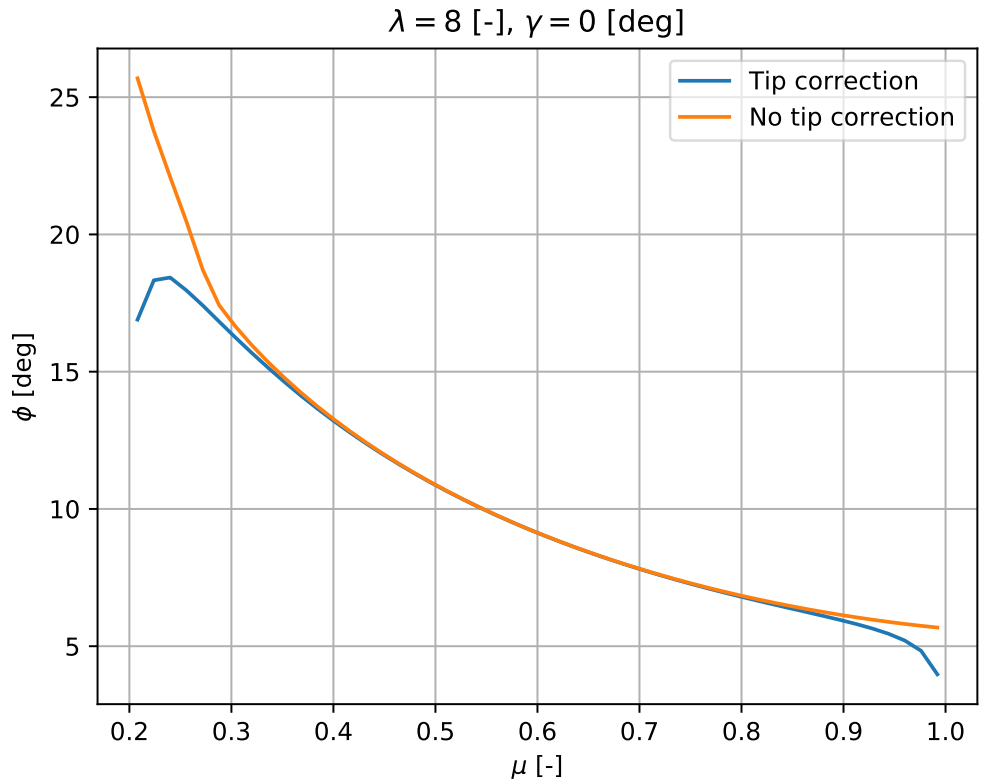

Figure 3.1: Flow angle distribution with and without tip correction.

3.4. Influence of numerical discretization BERNAT

3.5. Evaluation of stagnation enthalpy CARLOS

If heat exchange, viscous forces and compressibility effects are neglected, the flow temperature does not change. Therefore, it can be assumed that the air's internal energy is always constant. Then, the changes in stagnation enthalpy and stagnation pressure are equivalent. The mechanical energy equation (3.2) describes how the stagnation pressure p_t changes. Note that it has been obtained as the scalar product of the momentum equation and the velocity vector.

$$\vec{v} \cdot \vec{\nabla} p_t = \vec{v} \cdot \vec{\nabla} \cdot \vec{\vec{\tau}} + \vec{v} \cdot \vec{f} \tag{3.2}$$

If viscous forces are not considered, $\tau = 0$, the stagnation pressure can only due to the body forces b work. The only domain region where these forces are not null, and therefore, exert some work is

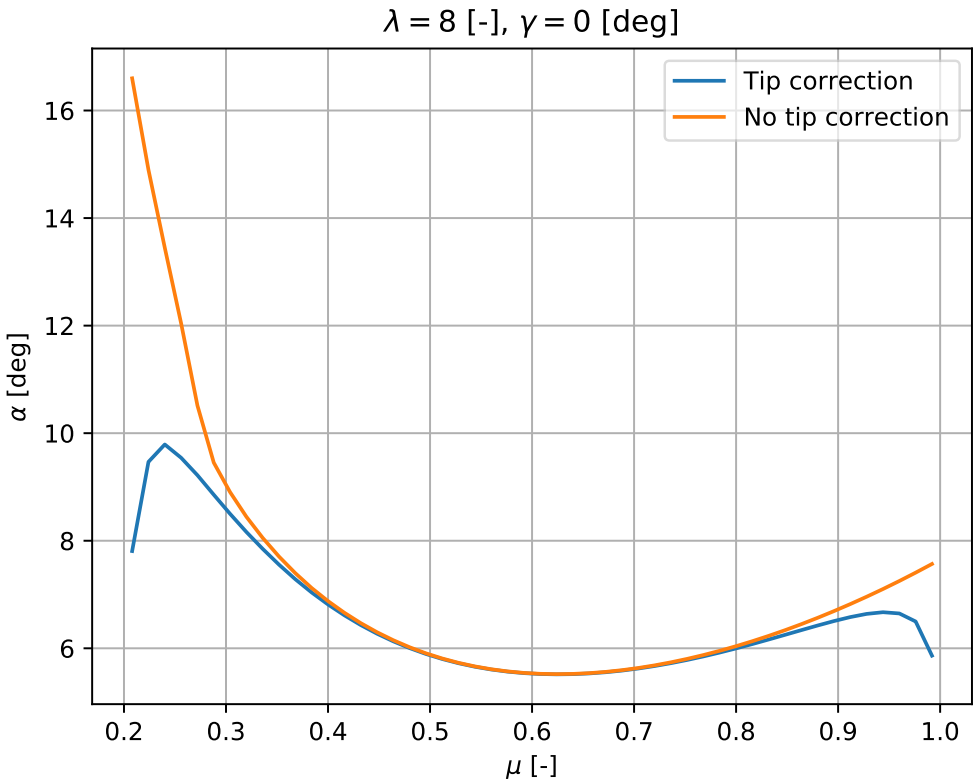

Figure 3.2: Angle of attack distribution with and without tip correction.

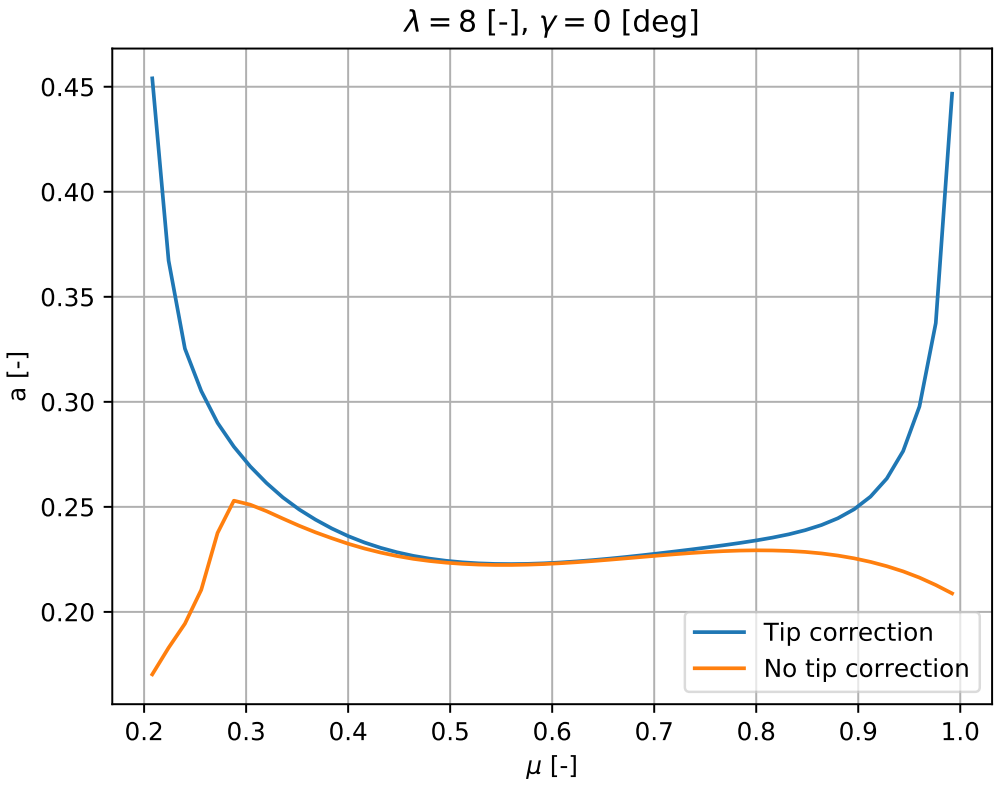

Figure 3.3: Axial induction distribution with and without tip correction.

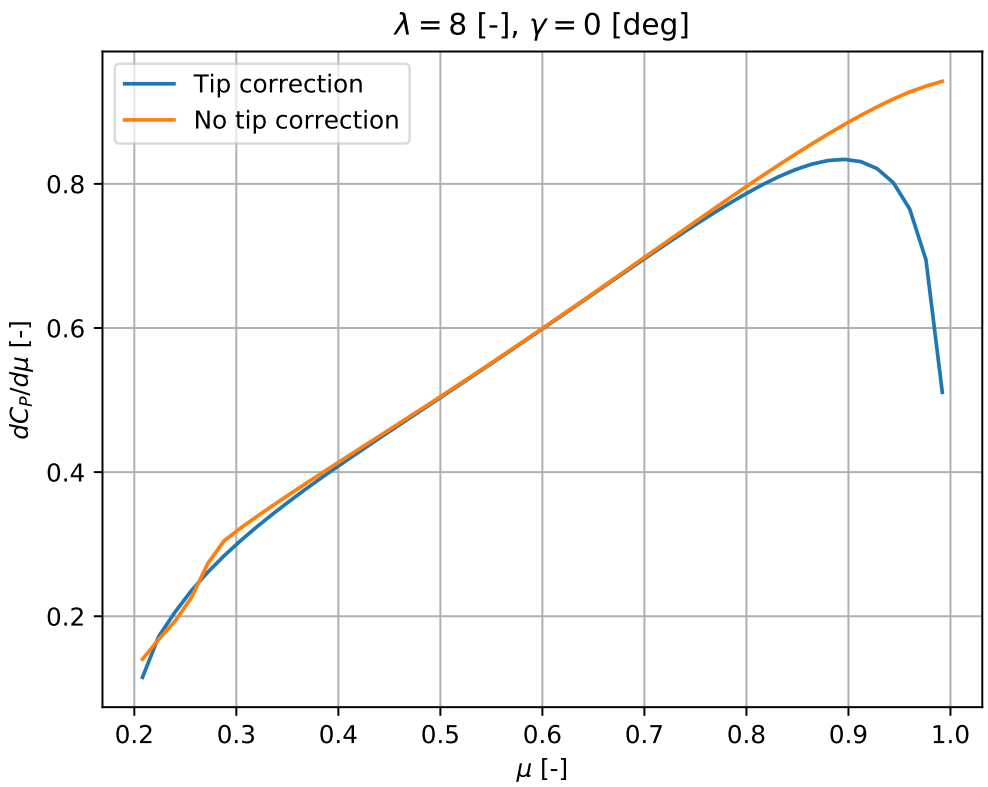

Figure 3.4: Power coefficient distribution with and without tip correction.

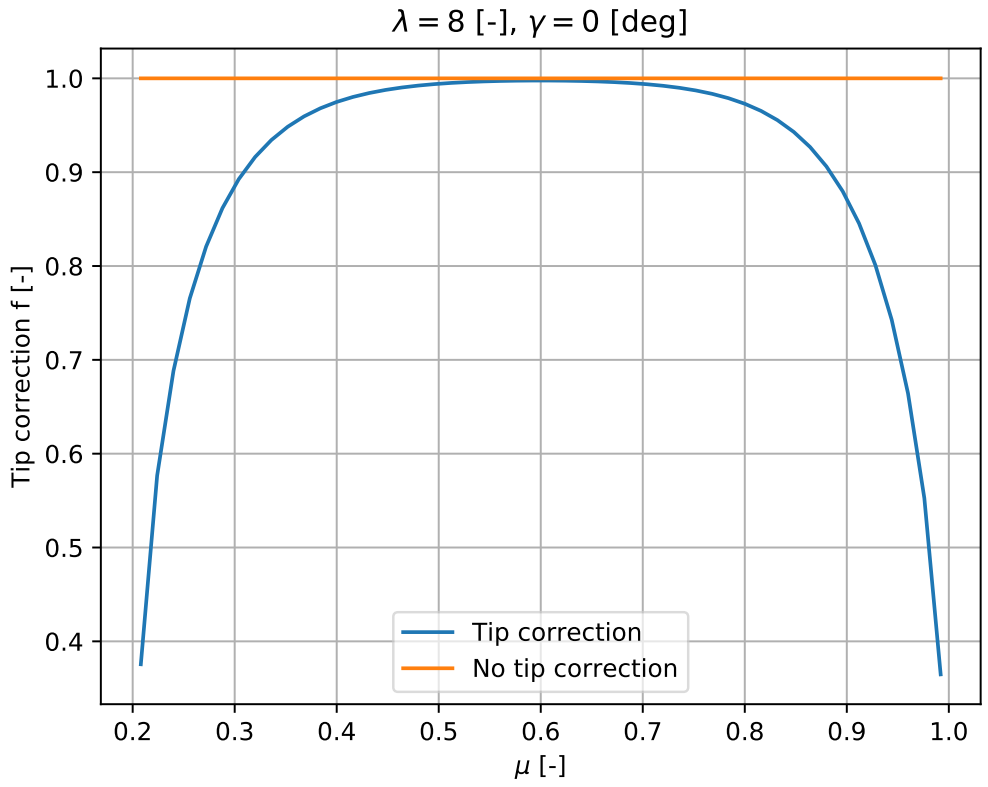

Figure 3.5: Prandtl's tip loss factor distribution with and without tip correction.

the rotor plane. This means that the stagnation pressure only changes across the rotor plane. See equations (3.3) and (3.4) for the stagnation pressure expressions up and down-stream of the rotor plane respectively. They are plotted in Figure 3.6.

$$p_{t_u} = p_a + \frac{1}{2}\rho u_\infty^2 \tag{3.3}$$

$$p_{t_d} = p_a + \frac{1}{2}\rho u_\infty^2 (1-2a)^2 \tag{3.4}$$

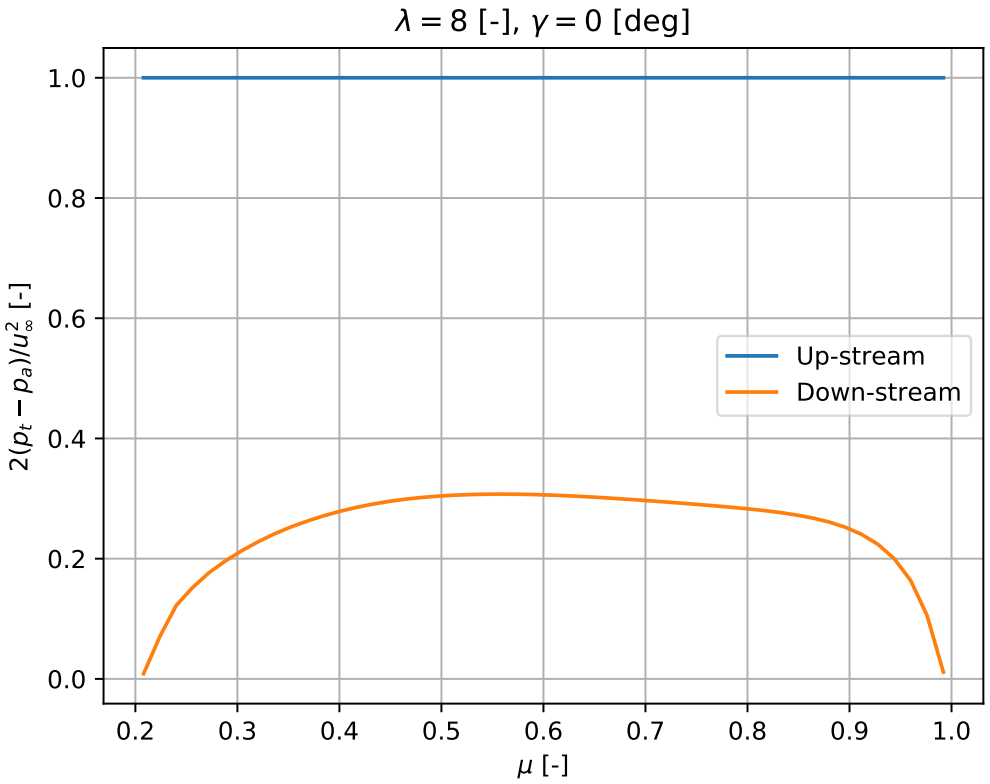

Figure 3.6: Stagnation enthalpy distribution.

3.6. System of circulation and vorticity CARLOS

The circulation distribution over the blade is shown in Figure 3.7. It has a more or less constant shape in the centre part of the blade, and vanishes quite steeply near the root and tip. This seems reasonable, since circulation is related to lift generation by the Kutta-Joukowski theorem: $l = \rho u_\infty \Gamma$. In the blade extremes, lift must be zero, since there is no surface that can create it.

The vorticity equation and Kutta-Jukowski theorem explain the changes observed in circulation. The thrust derivative with respect to the radius can be expressed using the Blade Element Theory, Kutta-Jukowski theorem and assuming no drag (3.5), or using the Momentum Theory (3.6).

$$\frac{dT}{dr} = l\cos\phi = \rho w \Gamma \cos\phi \tag{3.5}$$

$$\frac{dT}{dr} = \rho u_\infty (1-a) u_\infty 2a 2\pi r \tag{3.6}$$

If the expressions (3.5) and (3.6) are equated, it can be seen that the circulation is related to the local thrust. This is shown in Figure 3.8, where the two sides of equation (3.7) are plotted. The slightly

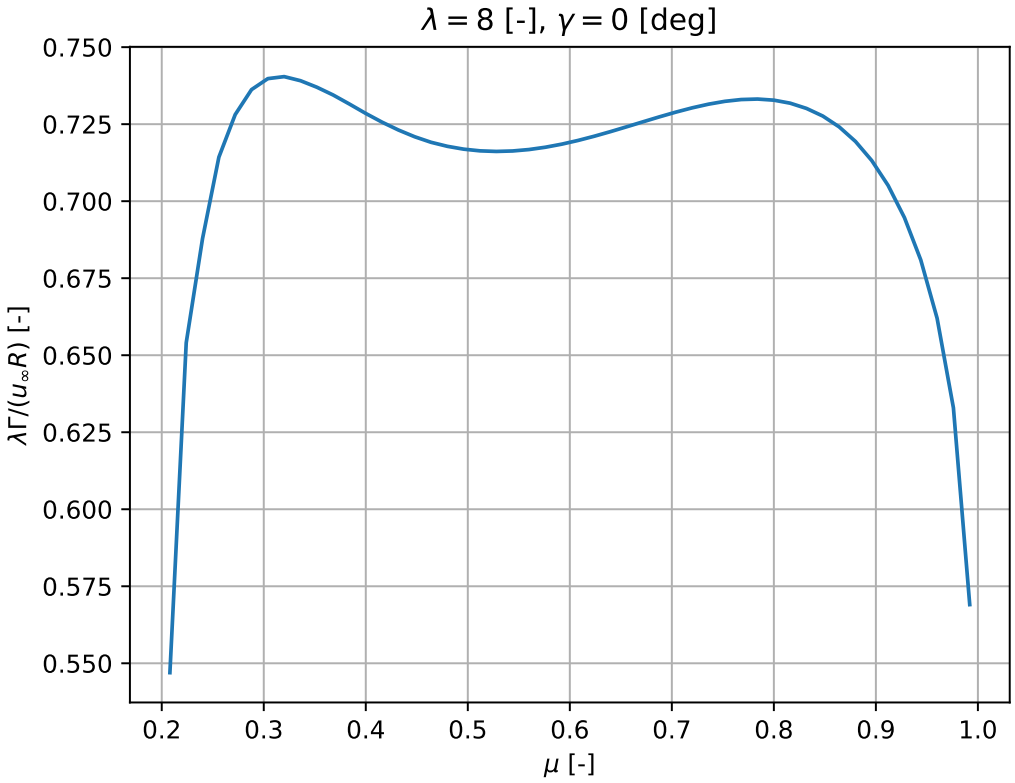

Figure 3.7: Circulation distribution.

higher values for the thrust coefficient may be due to the drag contribution, which is not accounted for in the circulation.

$$\frac{w\Gamma\cos\phi}{u_\infty^2\pi r} = 4a(1-a) = C_T \tag{3.7}$$

Equation (3.7) is actually a different form of the vorticity equation (3.8).

$$\vec{v}\cdot\vec{\nabla}\vec{\omega} = \vec{\nabla}\times\vec{f} \tag{3.8}$$

Assuming there are no radial forces, and that vorticity only changes in its direction ($d\omega_i/dx_j = 0$, if $i \neq j$), the vorticity equation in the tangential direction can be simplified to better show how it relates to expression (3.7).

$$w\cos\pi\frac{d\omega}{rd\theta} = -\frac{df_x}{dr} \tag{3.9}$$

If equation (3.9) is integrated over the volume, expression 3.7 is obtained. Remark that $\int 1/rd\omega/d\theta dV = -\int \omega dS = -\Gamma$, and $\int df_x/drdV = dT/dr$.

The same procedure can be done for the vorticity generation in the axial direction. In this case, the vorticity equation is the one shown in (3.10). The relationship between the circulation and tangential force is given by equation (3.11).

$$w\sin\pi\frac{d\omega}{dx} = \frac{df_\theta}{dr} \tag{3.10}$$

$$\frac{dS}{dr} = l\sin\phi = \rho w\sin\phi\Gamma = \rho u_\infty(1-a)\Omega r 2a' 2\pi r \tag{3.11}$$

The relationship between the tangential force and generation of circulation in the axial direction is depicted in Figure 3.9. The differences observed may be due to the drag, which reduces the tangential force created by the lift.

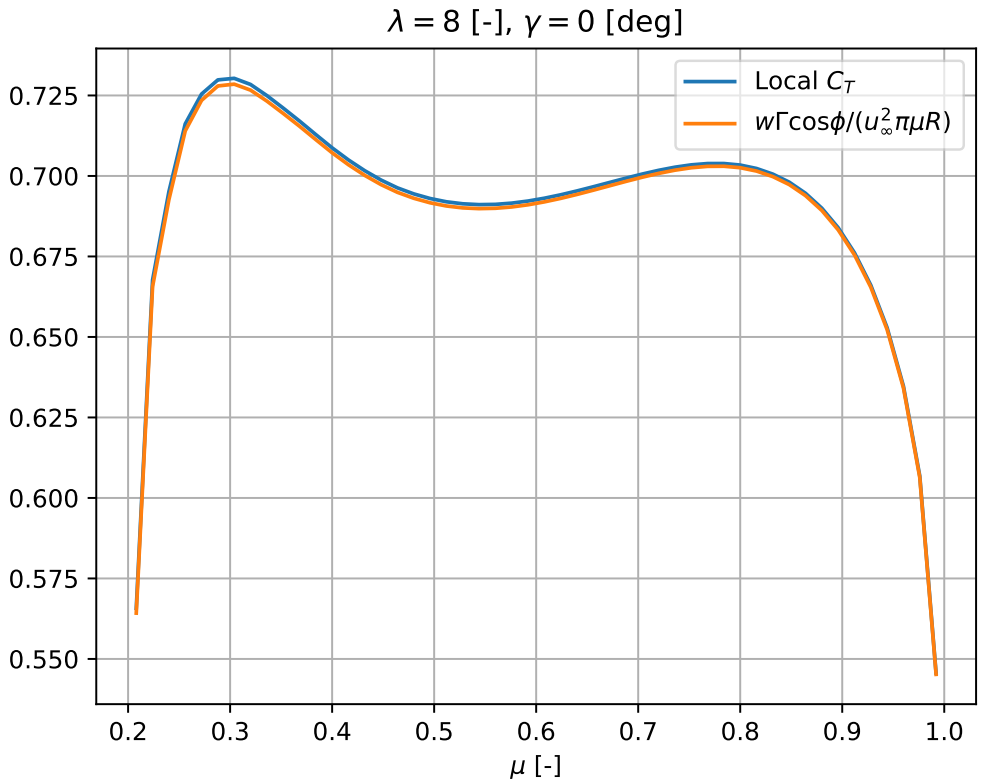

Figure 3.8: Circulation and local thrust coefficient distribution.

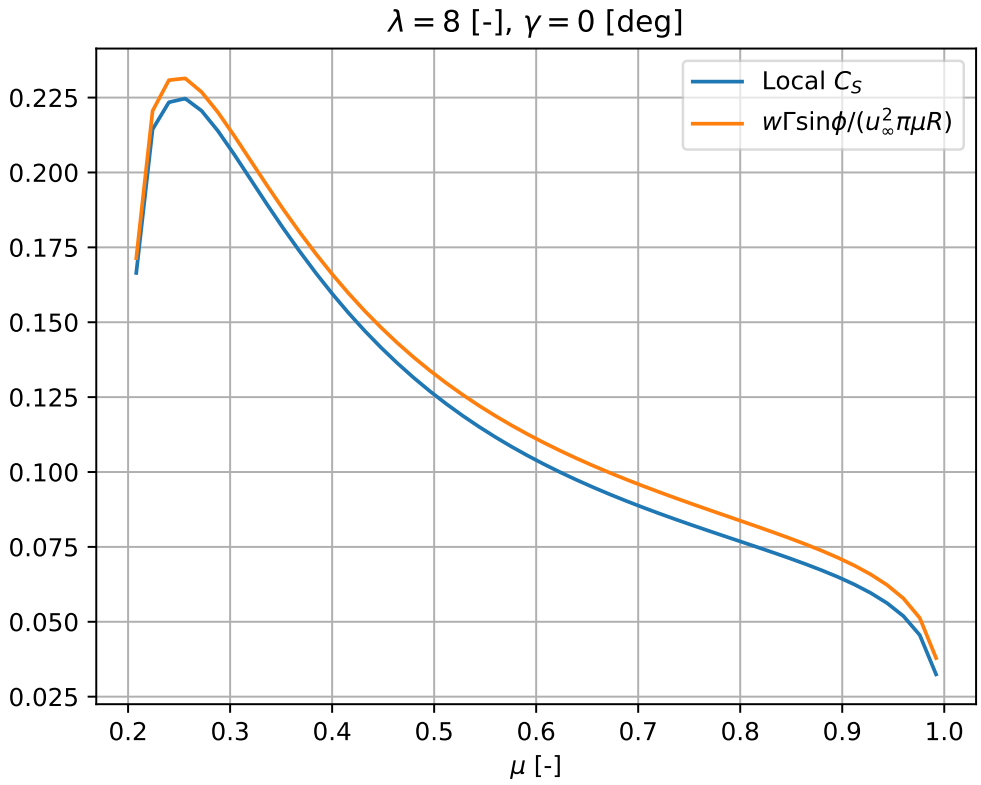

Figure 3.9: Circulation and local tangential coefficient distribution.

3.7. Operational point NIKLAS

4

Optional

4.1. Explanation of the design approach used for maximizing the Cp or efficiency

Blabla

4.2. Plots with explanation of the new designs

Rick Sanchez

5

Conclusions NIKLAS

SHORT discussion/conclusion, including the similarities and differences between the two rotor configurations (yaw vs. aligned rotor), flow field and operation

Bibliography

[1] Burton, T. and Jenkins, J. and Sharpe, D. and Bossanyi, E. *Aerodynamics of Horizontal Axis Wind Turbines*, chapter 3, pages 39–136. John Wiley & Sons, Ltd, 2011. ISBN 9781119992714. doi: https://doi.org/10.1002/9781119992714.ch3. URL https://onlinelibrary.wiley.com/doi/abs/10.1002/9781119992714.ch3.